ELECTROLESS NICKEL PLATING: PCB PROCESS MODELLING AND ESTIMATION

R. Tenno, K. Kantola and H. Koivo

Helsinki University of Technology,Control Engineering Laboratory,
P.O. Box 5500, FIN-02015 Espoo, Finland,
robert.tenno@hut.fi

1. INTRODUCTION

Electroless nickel plating is widely used process in many industries including printed circuit boards (PCB) where ultimately plating-through-hole (PTH) is applied. In this technology the product quality is controlled through the process chemistry using an automatic control system stabilising the nickel concentration and pH-index continuously. The set point for pH-index control is adjusted manually in dependence on the product quality and process state. This practical control is limited by a long delay of daily laboratory analysis and heuristic choice of the set point. It is shown in this paper that the PTH board quality can be estimated online and applied in fully automated control. This better control algorithm is based on the state estimation and application of the electrochemically balanced tracking trajectory calculated from a model developed in [1, 2] for conventional reaction mechanism [3]-[5].

2. MODEL

It was found in many studies [3-5, etc.] and confirmed in PTH process [1, 2] that an electroless nickel plating can be represented as the following system of anodic and cathodic reactions:

1. Anodic reaction - hypophosphite oxidation

$$H_2PO_3^- + 2H^+ + 2e^- \leftarrow H_2PO_2^- + H_2O, \qquad U_1 = -0.504\ V \qquad (1)$$

2. Cathodic reactions - phosphorous deposition, hydrogen evolution, nickel deposition

$$H_2PO_2^- + 2H^+ + e^- \rightarrow P + 2H_2O, \qquad U_2 = -0.391\ V \qquad (2)$$

$$2H^+ + 2e^- \rightarrow H_2, \qquad U_3 = 0\ V \qquad (3)$$

$$Ni^{2+} + 2e^- \rightarrow Ni. \qquad U_4 = -0.257\ V \qquad (4)$$

In these reactions, the hydrogen ion formation in bath exceeds consumption in product and for balancing a pH-control with ammonia is used

$$NH_3 + H_2O \leftrightarrow NH_4^+ + OH^-. \qquad (5)$$

Regardless to other processes, the discharge reaction controls the deposition process mainly. It can be represented as the following electrode reaction.

Electrode reaction. The current densities of the electrochemical reactions (1)-(4) can be represented as a two-directional process in a model, which is manly the anodic reaction model for oxidation and cathodic reaction model for others.

$$i_n = i_{0n}\mu_n\{\exp(\nu\alpha_{an}p_nk\eta_n) - \exp(-\nu\alpha_{cn}p_nk\eta_n)\}, \quad (6)$$

where
n - reaction number: 1 - oxidation, 2 - P deposition, 3 - hydrogen evolution, 4 - Ni deposition,
i_n - current density, A/cm^2,
i_{0n} - exchange current density, A/cm^2; i_{01} = 18, i_{02} = 0.5, i_{04} = 1.6 mA/cm^2; i_{03} is a constant i_{03} = 2.5 in [1] or a time-varying parameter in [6],
η_n - overpotential, $\eta_n = \phi - v_n$,
ϕ - mixed potential, V,
v_n - thermodynamic equilibrium potential, V,
μ_n - dimensionless concentration of species,
ν - robustness: empirical coefficient, 0.1,
k - temperature voltage, k = F/RT, 1/V,
T - temperature, K,
R - universal gas constant, 8.3145 J/mol-K,
F - Faraday's constant, 96487 C/mol,
p_n - number of exchanged electrons, p_2 = 1, other p_n = 2,
α_{an} - anodic apparent transfer coefficients, α_{a1}= 0.53, other $\alpha_{an} = 1 - \alpha_{cn}$,
α_{cn} - cathodic apparent transfer coefficients, α_{c2} = 0.62, α_{c3} = 0.59, α_{c4} = 0.47.

The anodic current density is equal to the sum of cathodic current densities (charge conservation)

$$i_1 + i_2 + i_3 + i_4 = 0. \quad (7)$$

The mixed potential is adjusted by the deposition process itself to maintain (7) irrespective to any changes in the concentrations or equilibrium potentials.

Equilibrium potential. The equilibrium potentials of the partial reactions can be evaluated from the Nernst equation of the partial reactions (1)-(4)

$$v_1 = U_1 + \kappa(\log c_5 - \log c_1 - 2pH), \quad (8)$$

$$v_2 = U_2 + 0.2\kappa(\log c_1 - 2pH), \quad (9)$$

$$v_3 = U_3 - 2\kappa\, pH, \quad (10)$$

$$v_4 = U_4 + \kappa \log c_4, \quad (11)$$

where κ^{-1} = 2k log e, c_i - ion concentration of species, mol/dm^3.

Concentration controlled electrode. The current densities are concentration controlled through the equilibrium and mixed potentials and through the following limitation and activation coefficients found experimentally

$$\mu_1 = \frac{c_1}{0.7c_1 + 0.3c_{1ref}}, \qquad \mu_2 = 0.5\left[1+\frac{c_{3ref}}{c_3}\right]\left[1+0.1\frac{c_5}{c_{5max}}\right], \tag{12}$$

$$\mu_3 = \frac{c_3}{0.6c_3 + 0.4c_{3ref}}\left[1+0.1\frac{c_5}{c_{5max}}\right], \qquad \mu_4 = \frac{c_4}{c_{4ref}}\left[0.6+0.4\frac{c_{3ref}}{c_3}\right], \tag{13}$$

where $c_{i.ref}$ - reference concentration of species (concentration after makeup), mol/dm^3.

Plating. The deposition process can be decomposed in two independent processes - in nickel and phosphorous deposition processes and composed by superposition for calculation of the Ni-P-alloy film $x_a = x_{Ni} + x_P$.

$$\frac{dx_{Ni}}{dt} = -i_4\frac{M_{Ni}}{2F\rho_{Ni}}, \qquad \frac{dx_P}{dt} = -i_2\frac{M_P}{F\rho_P}, \tag{14}$$

where

t - immersion time, sec,

x_{Ni} - partial thickness of nickel (ratio between nickel volume and plate area), cm,

x_P - partial thickness of phosphorous, cm,

x_a - thickness of the Ni-P-alloy film, cm,

i_4 - current density of nickel deposition reaction, A/cm^2,

i_2 - current density of phosphorous deposition reaction, A/cm^2,

M - molecular weight of nickel M_{Ni} = 58.7 g/mol or phosphorous M_P = 31 g/mol,

ρ - density of nickel ρ_{Ni} = 8.9 g/cm^3 or phosphorous ρ_P = 1.82 g/cm^3.

The phosphorous content in film can be expressed as a volumetric ratio between the overall and partial thicknesses $P_{vol} = (x_P/x_a)100\%$ or as a weight ratio P_{wt} between the overall and partial weights.

Concentration dynamics. Feeding and utilization of the reagents along with formation of the by-products induces coupled changes of the concentrations of species.

1. Hypophosphite feeding and consumption

$$dc_1 = [A(2i_2 - i_1)/2F + Q_{1f}c_{1f}]dt + \sigma_1 dW, \qquad c_1(t_0) = c_{1ref}, \tag{15}$$

where

c_1 - hypophosphite concentration, mol $H_2PO_2^-$/dm^3,

c_{1f} - feeding solution concentration, mol $H_2PO_2^-$/dm^3,

Q_{1f} - hypophosphite dilution rate, 1/s,

A - bath loading, cm^2/dm^3,

t_0 - makeup moment for a newly made bath, sec,

t - elapsed time, sec,

σ_1 - model inaccuracy,

W - model-prediction error: Wiener process.

2. Nickel feeding and consumption

$$dc_4 = [Ai_4/2F + Q_{4f}\, c_{4f}]dt + \sigma_4 dW, \quad c_4(t_0) = c_{4ref}, \tag{16}$$

where
c_4 - nickel concentration, mol Ni^{2+}/dm^3,
c_{4f} - feeding solution concentration, mol Ni^{2+}/dm^3,
Q_{4f} - nickel dilution rate, 1/s.

3. Hydrogen formation and removal with ammonia

$$dc_3 = [A(i_1 + 2i_2 + i_3)/F - Q_{3f}c_{3f}]dt + \sigma_3 dW, \quad c_3(t_0) = c_{3ref}, \tag{17}$$

where
c_3 - hydrogen concentration, mol H^+/dm^3,
c_{3f} - ammonia concentration, mol NH_3/dm^3,
Q_{3f} - ammonia dilution rate, 1/s.

Accumulation of the by-products and the gas evolution can be represented as follows.

4. Orthophosphite accumulation

$$dc_5 = Ai_1 dt/2F + \sigma_5 dW, \qquad c_5(t_0) = 0, \tag{18}$$

c_5 - orthophosphate concentration, mol $H_2PO_3^-/dm^3$.

5. Hydrogen evolution

$$dc_6 = -Ai_3 dt/2F + \sigma_6 dW, \qquad c_6(t_0) = 0, \tag{19}$$

dc_6/dt - hydrogen gas evolution rate, mol $gH_2/s/dm^3$.

Measurements. A relatively complete data are required for model calibration and accuracy analysis. For these purposes, the following set of data was used.

1. Nickel percentage.
2. pH-index.
3. Nickel, hypophosphite and ammonia feeding rates.
4. Bath temperature.
5. Plating time.
6. Record of the bath loading events.
7. Mixed potential versus standard hydrogen electrode.
8. Hypo- and orthophosphite molar concentrations.
9. Thickness of plating film measured using X-ray fluorescence analyser.
10. Phosphorous content measured using scanning electron microscope.

Less data are required for control and online monitoring of the unobservable processes. In dependence on process automation level two sets of data may be used.

- Advanced PCB process [1, 2]

  1. Nickel percentage.
  2. pH-index.
  3. Nickel, hypophosphite and ammonia feeding rates.
  4. Bath temperature.
  5. Plating time.
  6. Bath loading events.
  7. Mixed potential.

- Conventional PCB process [6]

  1. Nickel percentage.
  2. pH-index.
  3. Nickel, hypophosphite and ammonia feeding rates.
  4. Bath temperature (constant).
  5. Plating time (constant).

3. MODEL ACCURACY

The electrode reaction model (6) with limitation/activation coefficients (12), (13) was calibrated using data measured during industrial experiment. In this experiment, the PTH process was changed in wide range of variables admissible by production technology. The calibrated model was then tested against the data measured in experiment 1 and new data measured in experiments 2, 3. Also unobservable processes were estimated using these data. The model accuracy evaluated from comparison with the measured data is shown in Figs 1-4. The model predicted Ni-P-alloy film is compared with the measured thickness in Fig. 1 and phosphorous content with the measured content in Fig. 2.

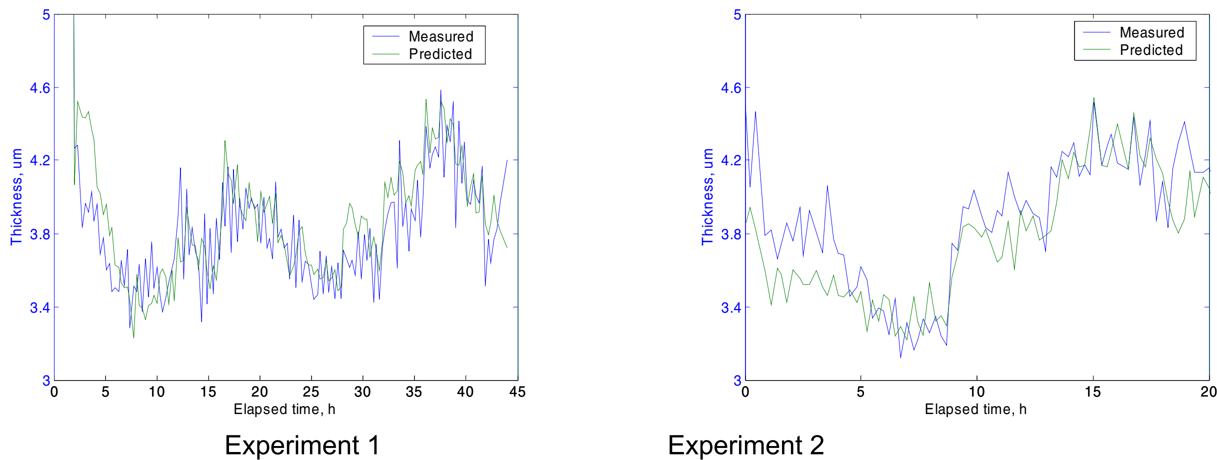

Fig. 1. Measured and predicted thickness of Ni-P-alloy film.

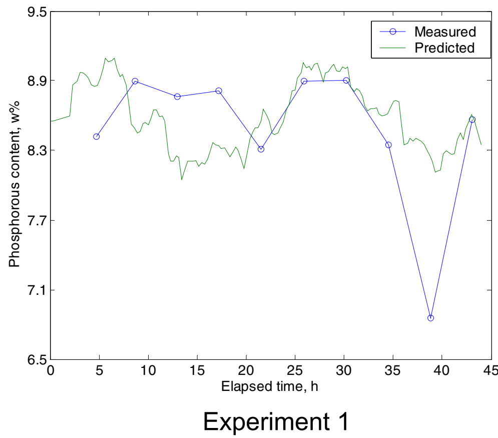

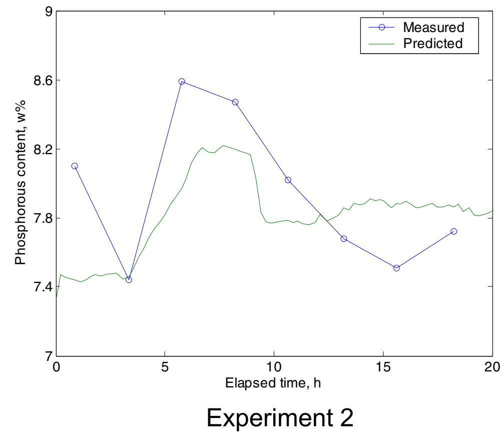

Fig. 2. Measured and predicted phosphorous content in film.

The deposition speed calculated by the data measured in the experiment is compared with the model in Fig. 3.

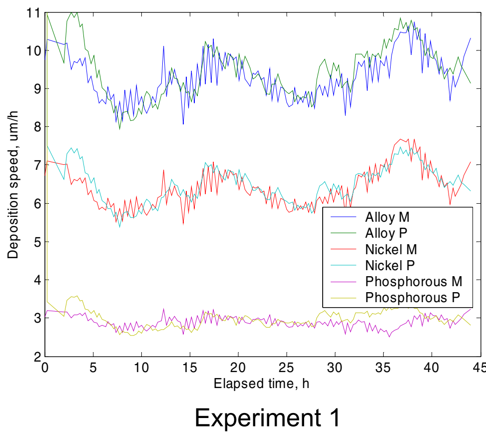

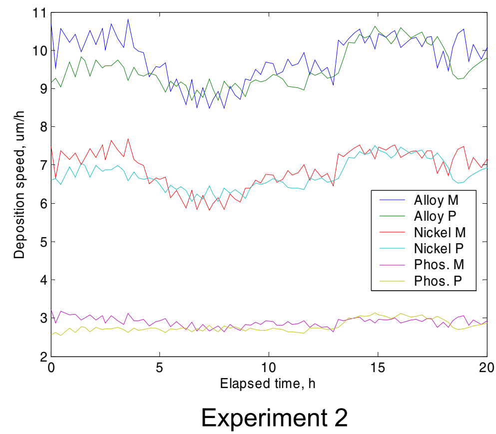

Fig. 3. Measured (M) and predicted (P) deposition speed of alloy, nickel and phosphorous.

The nickel percentage and pH-index are measurable processes; their prediction is not required for monitoring or control but is shown in Fig. 4 as a good indicator of the model accuracy as depends on many processes.

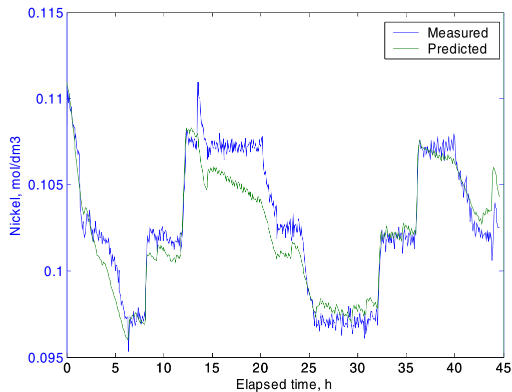

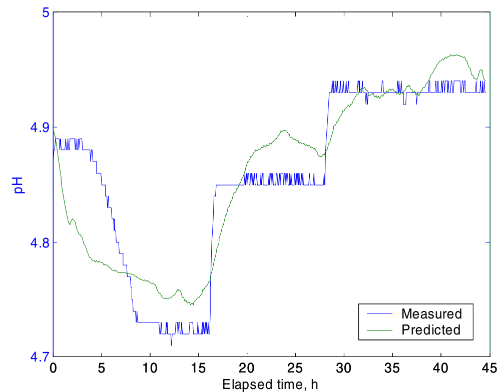

Fig. 4. Measured and predicted nickel concentration and pH-index.

Passive experiment. Some more evidence on the model accuracy was obtained in a long-term observation in passive experiments 3 and 4. These data shown in Figs 5, 6 are compared with the model. Note, that the mixed potential and bath loading processes were not available for the model calculation by the data observed in these experiments. The mixed potential was estimated from the continuity requirement (7) and the loading process from a Markov model developed specially for the loading process estimation in [6].

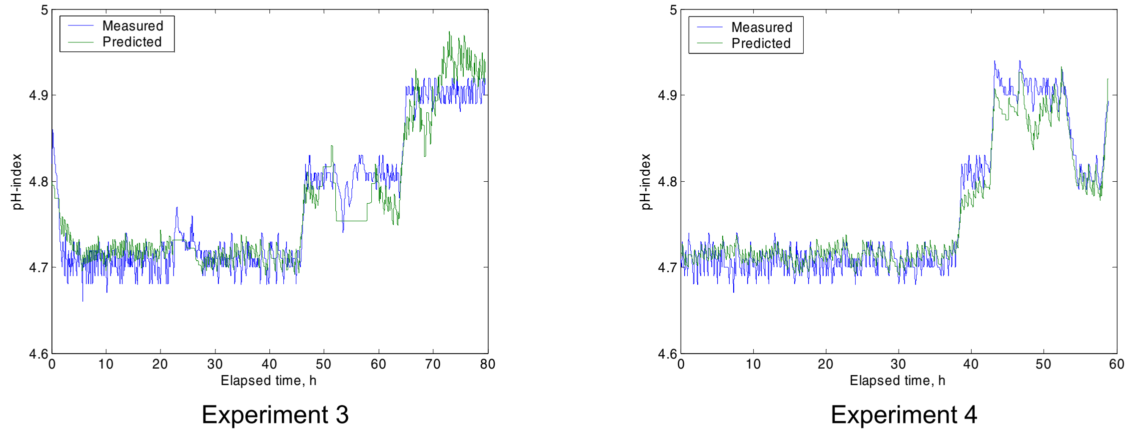

Fig. 5. Measured and predicted pH-index in passive experiment.

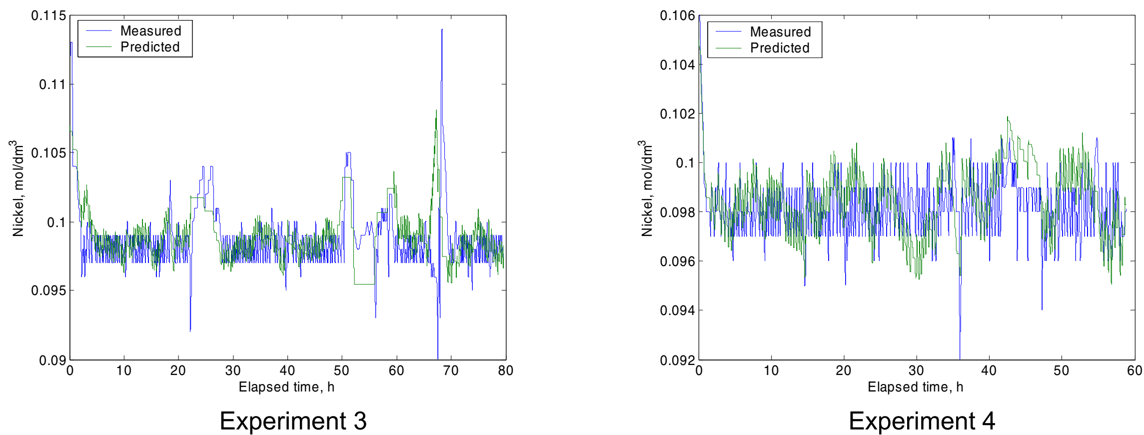

Fig. 6. Measured and predicted nickel concentration in passive experiment.

Summary. The model accuracy evaluated in the industrial experiment is summarized in Table 1, where Data 1 represents the model calibration data and Data 2, 3 - two new experiments with different values for the metal turn over (MTO). The model accuracy is exposed as a standard deviation of the predicted and measured processes; it is exposed in normalized unit as a percentage from the admissible by production technology range.

Table 1. Model accuracy.

Parameter	Admissible range	Accuracy, %			
		Data 1	Data 2	Data 3	Data 1 - 3
MTO	1 – 6	1 - 2	2 - 3	3 - 4	1 - 4
Film thickness	2.5 - 5 μm	9	17	9	12
Phosphorus	7 - 10 %	18	16	10	15
Nickel	90 – 105 %	9	10	7	9
pH-index	4.2 - 5.3	3	2	5	3

4. PCB PROCESS MONITORING

Most of the PCB processes can be estimated online by the measurable processes using the model (6)-(17). Some of these processes are shown in Figs 7-10. The film thickness, equilibrium and mixed potentials, current densities and reaction rates estimated by observable processes are shown in these figures.

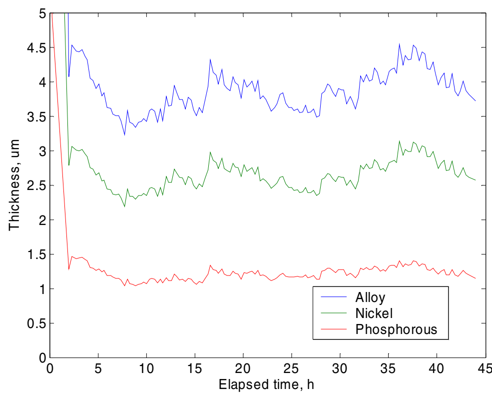

Fig. 7. Thickness of Ni-P-alloy film and partial thicknesses of nickel and phosphorous.

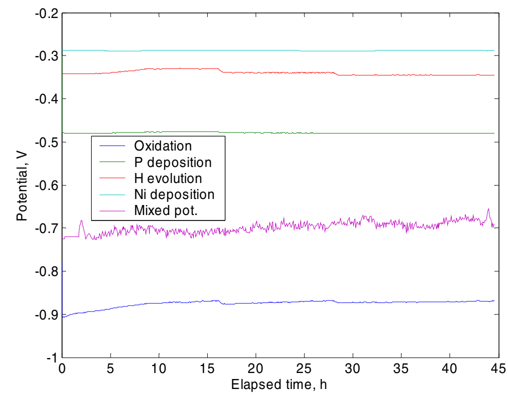

Fig. 8. Mixed and equilibrium potentials.

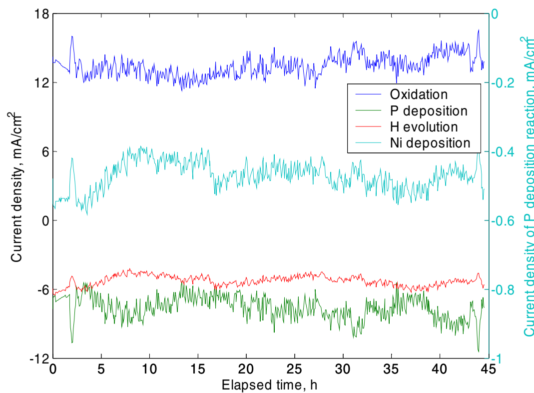

Fig. 9. Current densities of partial reactions.

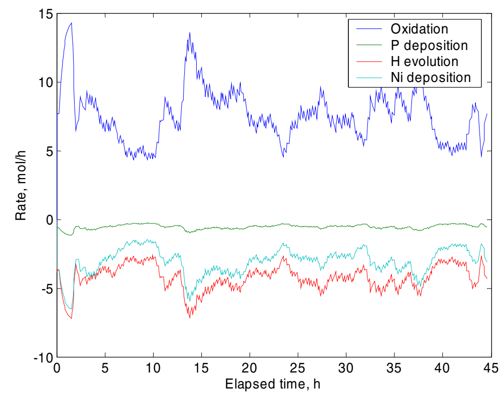

Fig. 10. Reaction rates.

5. CONTROL

The thickness and phosphorous content of plating film are crucial parameters of final quality of PCB. They can be kept at desired level through control of the ammonia and hypophosphite/nickel feeding rates.

In practice, a regulator is set up to stabilize the nickel percentage at constant level and pH-index at variable level, which depends on experience of operator to use effectively the laboratory analysis (film thickness, IPC-tape test) measured once per day.

In precise control, the target level for thickness $x_a = 4$ μm and phosphorous content $P_{wt} = 8.5$ % can be maintained by stabilization of the nickel concentration and pH-index at target level, which depends on process state.

Balanced trajectory. The target level for thickness and phosphorous can be achieved if an electrochemically balanced tracking trajectory is used for adjustment of the pH-index and nickel percentage along with corresponding trajectory of the mixed potential. This triple is attainable if satisfies the electrochemical system, which includes the charge conservation requirement (7) and the deposition rate (14) requirements derived from targets x_a = 4 μm, P_{vol} = 32 % as

$$- i_4 \frac{M_{Ni}}{2F\rho_{Ni}} T = x_{Ni}, \qquad - i_2 \frac{M_P}{F\rho_P} T = x_P, \tag{20}$$

where
x_{Ni} - target thickness of nickel, x_{Ni} = 4E-4 - x_P, cm,
x_P - target thickness of phosphorous, $x_P = 0.32\, x_a$, cm,
T - plating time (22-25 min), s.

Numerically, the balanced trajectory $\{c_3, c_4, \phi\}$ can be calculated by minimisation of the function

$$f = (i_1 + i_2 + i_3 + i_4)^2 + (i_2 - x_P \frac{F\rho_P}{TM_P})^2 + (i_4 - x_{Ni} \frac{2F\rho_{Ni}}{TM_{Ni}})^2, \tag{21}$$

composed of the charge conservation (7) and thickness requirements (20).

Therefore, the balanced trajectory is a triple of the hydrogen (pH-index), nickel concentrations and mixed potential calculated from (21) in dependence on the hypo- and orthophosphite concentrations

$$\zeta_3 = c_3(c_1,c_5), \qquad \zeta_4 = c_4(c_1,c_5), \qquad \phi = \phi(c_1,c_5).$$

In the partially observable case [6], they are calculated based on estimated values.

The plating process is well controllable as far as this relationship between target values holds. Otherwise an automatic change of the mixed potential takes place effecting all reactions. Unfortunately, this change takes place always even if the pH-index and nickel percentage are constants. The hypo- and orthophosphite concentrations are never constants, beside the feeding rates they depend on the utilization and consumption rates. The orthophosphate consumption similar to the MTO characterizes change of bath chemistry in aging.

Therefore, the thickness and phosphorous content of plating film can be maintained at the desired level through stabilization of the pH-index and nickel percentage at certain time-varying levels. This is a tracking control problem solved as follows.

Bath control. The thickness and phosphorous content can be kept at a desired level through tracking of the optimal trajectories for the pH-index and nickel percentage. The following feed-forward PI-control solves this problem approximately

$$u_t = x_t\nu - K_p[\xi_t - \zeta_t + T_i^{-1}\int_0^t (\xi_s - \zeta_s)ds], \tag{22}$$

where
ζ - electrochemically balanced tracking trajectory, $\zeta = [\zeta_3, \zeta_4]^T$,
ξ - measured nickel concentration and hydrogen concentration, $\xi = [c_3, c_4]^T$,
u - controls: ammonia and hypophosphite/nickel feeding rates, $u = [Q_{3f}, Q_{4f}]^T$,

x_t - state of bath loading: measured [1] or estimated [6],
ν - setpoint for controls,
K_p - regulator gain: diagonal matrix of weights,
T_i - integration time.

This simple control law depends on the model through tracking level and also on loading if the loading level is unobservable process [6]. This law was tested against many loading profiles, which show that the PTH process can be stabilized irrespective to any changes in loading. This control is effective because of the following properties.

1. The electrochemically balanced tracking trajectory is relevant to the global target and to the current state of process.

2. The state of bath loading switches controls faster than its after effect measured pH-index or nickel percentage can do.

3. The nickel concentration tracking allows separate control of the film thickness and phosphorous content. Otherwise, their control is in disagreement if single control (pH-index) is applied.

6. SIMULATION

The control effect is demonstrated in the following simulation experiment, where initially low thickness 3.75 μm and phosphorous content 7.85 % was corrected up to the target values x_a = 4.5 μm, P_{wt} = 8.5 % irrespective to the loading changes between zero and maximum values. The bath loading process was simulated as a Markov pure jump process in Fig. 11 and then filtered from the pH-index and nickel percentage as a least-squares estimate [6].

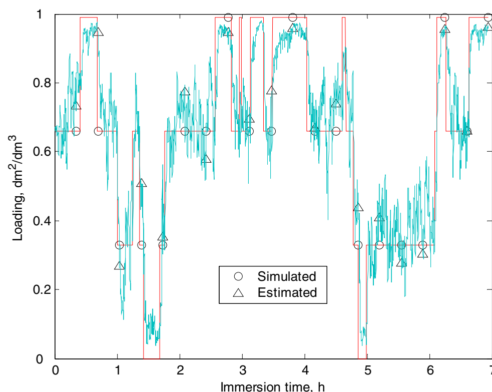

Fig. 11. Simulated and estimated bath loading.

Irrelevant to loading, the film thickness and phosphorous content can be stabilised at target levels rather well shown in Figs 12, 13.

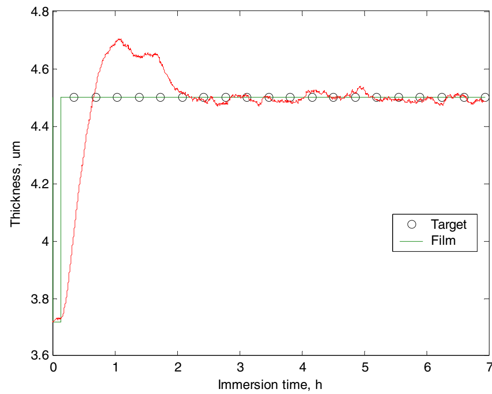

Fig. 12. Stabilised thickness.

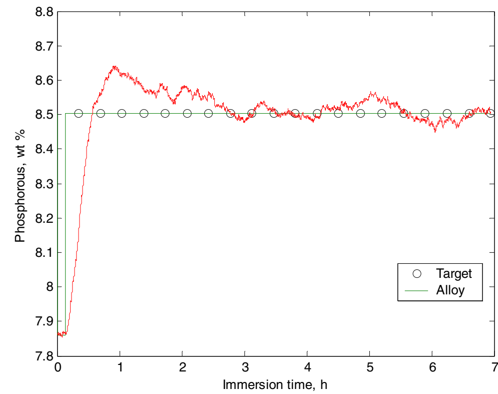

Fig. 13. Stabilised phosphorous.

The initial state correction is the biggest one. It affects on the deposition rates (Fig. 14) and also on the rate-ratios to achieve the desired thickness and phosphorous content.

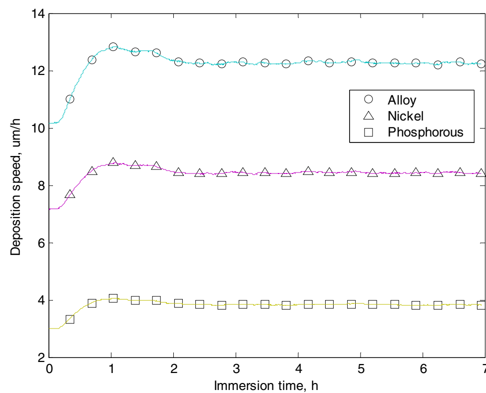

Fig. 14. Corrected deposition speed.

The electrochemically balanced trajectory is not far from average in a long run but its deviation is systematic in a short run (Fig 15).

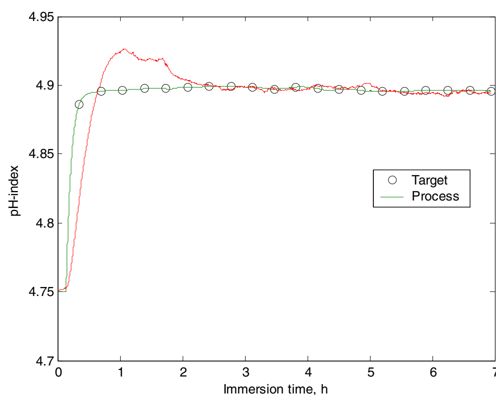

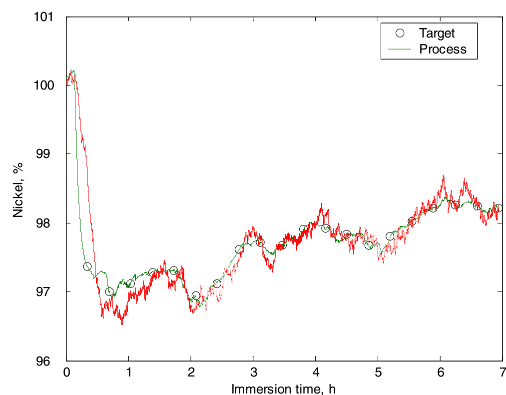

Fig. 15. Electrochemically balanced tracking trajectory for pH-index and nickel concentration, and their real tracking in process control.

Small changes of the feeding rates are required to stabilise the plating process if correction is made in time and both flows are active controls.

In the case of conventional PID control, variation is essentially larger because the desired pH-index and nickel concentration are never balanced. To prevent unstable situations a piece-wise constant pH-trajectory is aimed for tracking in practice while the nickel concentration level is aimed for keeping the level constant.

8. CONCLUSION

The industrial PTH process was predicted with model and its unobservable state was estimated online using measured results of standard analyzers also when the mixed potential and bath loading measurements were missing. Therefore, the state of PCB process could be characterized in terms of the electrochemical and chemical parameters and controlled online. The control quality could be improved considerably compared to the commonly used control.

LITERATURE

[1] Tenno R., K. Kantola, H. Koivo, A. Tenno. Model for electroless nickel plating through hole boards. AIChE J. (submitted)

[2] Kantola K., R. Tenno, H. Koivo. Model prediction accuracy for electroless nickel plating through hole boards. *AIChE* J. (submitted)

[3] Paunovic M., M. Sclesinger. *Fundamentals of electrochemical deposition.* John Wiley & Sons, Inc. 1998. 301 pp.

[4] Mallory G.O. The fundamental aspects of electroless nickel plating in *Electroless plating: fundamentals and applications.* Ed. Mallory G.O., Hajdu J.B. AESF Society. Orlando. 1990. P. 1-56.

[5] Kim Y.-S., H.-J. Sohn. Mathematical modelling of electroless nickel deposition at steady state using rotating disk electrode. J. *Electrochem. Soc.* Vol 143, No 2. 1996. P. 505-509.

[6] Tenno R., H. Koivo, A. Tenno. Partially observable nickel plating control. IFAC J. *Process Control.* (submitted)